BIOCHEMISTRY
including biophysical chemistry & molecular biology
Article

Biochemistry **2009,** *48,* 6655–6663 6655
DOI: 10.1021/bi9007403

Structure-Dependent DNA Damage and Repair in a Trinucleotide Repeat Sequence[†]

Daniel A. Jarem, Nicole R. Wilson, and Sarah Delaney*

Department of Chemistry, Brown University, Providence, Rhode Island 02912

Received April 29, 2009; Revised Manuscript Received June 5, 2009

ABSTRACT: Triplet repeat sequences, such as CAG/CTG, expand in the human genome to cause several neurological disorders. As part of the expansion process the formation of non-B DNA conformations by the repeat sequence has previously been proposed. Furthermore, the base excision repair enzyme 7,8-dihydro-8-oxoguanine glycosylase (OGG1) has recently been implicated in the repeat expansion [Kovtun, I. V., Liu, Y., Bjoras, M., Klugland, A., Wilson, S. H., and McMurray, C. T. (2007) *Nature 447*, 447−452]. In this work we have found that the non-B conformation adopted by $(CAG)_{10}$, a hairpin, is hypersusceptible to DNA damage relative to the $(CAG)_{10}/(CTG)_{10}$ duplex and, in particular, that a hot spot for DNA damage exists. Specifically, we find that a single guanine in the loop of the hairpin is susceptible to modification by peroxynitrite. Interestingly, we find that human OGG1 (hOGG1) is able to excise 7,8-dihydro-8-oxoguanine (8-oxoG) from the loop of a hairpin substrate, albeit with a marked decrease in efficiency relative to duplex substrates; the hOGG1 enzyme removes 8-oxoG from the loop of a hairpin with a rate that is ∼700-fold slower than that observed for DNA duplex. Thus, while damage is preferentially generated in the loop of the hairpin, DNA repair is less efficient. These observed structure-dependent patterns of DNA damage and repair may contribute to the OGG1-dependent mechanism of trinucleotide repeat expansion.

The pathogenic element of at least eight neurodegenerative disorders, including Huntington's disease (HD),[1] has been pinpointed as the expansion of a CAG/CTG trinucleotide repeat sequence (*1*). In all CAG/CTG trinucleotide repeat disorders the repeat sequence occurs in a protein-coding region, and therefore, gene expression results in a protein product with an expanded glutamine tract (*2*). The function of the normal HD protein remains an active area of research; however, it is known that the mutant HD protein, which harbors a tract of more than 40 glutamine residues, has aberrant properties that cause the death of brain cells (*3*). Indeed, it is the death of these cells that leads to both the mental decline and uncoordinated body movements associated with HD and other trinucleotide repeat disorders.

Proposed mechanisms for the DNA trinucleotide repeat expansion include polymerase slippage during a postrepair event or during replication of the repeat sequence (*4*). The slippage event is thought to be facilitated by the formation of stable non-B conformations by the repetitive CAG and/or CTG sequences (*5*). Indeed, *in vitro* studies using optical melting analysis, differential scanning calorimetry, NMR, circular dichroism, and chemical probes of nucleobase accessibility have shown that single strands of DNA containing a repetitive CAG or CTG sequence form intramolecular hairpins (*6*−*8*).

Additionally, recent studies in mice have implicated the base excision repair enzyme 7,8-dihydro-8-oxoguanine glycosylase (OGG1) in the CAG/CTG repeat expansion (*9*). OGG1 initiates the base excision repair (BER) process in mammalian cells by excising oxidized bases from duplex DNA, with 7,8-dihydro-8-oxoguanine (8-oxoG) being the prototypic and most well studied substrate (*10*). Following the removal of 8-oxoG by the glycosylase activity of OGG1, which generates an apurinic (AP) site, the β-lyase activity of OGG1 converts the AP site to a strand break (*11*). The consecutive actions of several other enzymes, including AP endonuclease 1 (APE1), polymerase β (pol β), and DNA ligase, fill the single base gap and complete the repair event. Indeed, this BER process has been reconstituted *in vitro* using 100 base pair duplex substrates containing a site-specific 8-oxoG lesion either flanked on both sides by mixed-sequence DNA or flanked by mixed-sequence DNA to the 5′-side and $(CAG)_{19}/(CTG)_{19}$ to the 3′-side. It has been shown that the BER repair event is faithfully completed when the 8-oxoG lesion is surrounded by mixed sequence but that products greater than 100 base pairs are observed when the CAG/CTG repeat region is present (*9*). Thus, OGG1 can initiate trinucleotide repeat expansion during the gap-filling step of BER.

[†]This work was supported by Brown University in the form of start-up funds and a Richard B. Salomon Faculty Research Award to S.D. D.A.J. acknowledges the Department of Education for a GAANN Fellowship.

*To whom correspondence should be addressed. Telephone: (401) 863-3590. Fax: (401) 863-9368. E-mail: sarah_delaney@brown.edu.

[1]Abbreviations: 8-oxoG, 7,8-dihydro-8-oxoguanine; AP, apurinic; APE1, apurinic endonuclease 1; BER, base excision repair; BSA, bovine serum albumin; DEPC, diethyl pyrocarbonate; DMT, dimethoxytrityl; EDTA, ethylenediaminetetraacetic acid; HPLC, high-performance liquid chromatography; HD, Huntington's disease; IPTG, isopropyl β-D-thiogalactoside; LB, Luria−Bertani broth; OGG1, 7,8-dihydro-8-oxoguanine glycosylase; PAGE, polyacrylamide gel electrophoresis; PMSF, phenylmethanesulfonyl fluoride; pol β, polymerase β; TBE, Tris−borate−EDTA; T_m, melting temperature; TNR, trinucleotide repeat; Tris, tris(hydroxymethyl)aminomethane.

Published on Web 06/15/2009

Here, given the proposed roles for oxidative DNA damage and repair in trinucleotide repeat expansion, we examined the susceptibility of the CAG/CTG repeat sequence to an oxidizing agent. We find that the trinucleotide repeat sequence is susceptible to modification by a solution-borne reactive species when in a hairpin conformation, in particular, in the loop of the hairpin; however, when present as a duplex, the CAG/CTG trinucleotide repeat sequence is protected from modification. Interestingly, despite preferential accumulation of damage at this site, we find that the rate of removal of 8-oxoG from the loop of a hairpin by human OGG1 (hOGG1) is ~700-fold slower than from duplex substrates.

EXPERIMENTAL PROCEDURES

Oligonucleotide Synthesis and Purification. Oligonucleotides were synthesized using standard phosphoramidite chemistry (*12*) on a BioAutomation DNA/RNA synthesizer. For the oligonucleotides containing 8-oxoG two rounds of HPLC purification were performed using a Dionex DNAPac PA100 anion-exchange column (4 × 250 mm) using 10% acetonitrile (aq) (solvent A) and 0.8 M ammonium acetate in 10% acetonitrile (aq) (solvent B) as the mobile phases (gradient: solvent B was increased from 30% to 55% over 10 min, then 55% to 75% over 10 min, and 75% to 90% over 19 min; 1 mL/min).

For the synthesis of the oligonucleotides lacking 8-oxoG the 5′-dimethoxytrityl (DMT) group was retained to facilitate purification. HPLC purification of these oligonucleotides was performed on a Dynamax Microsorb C18 column (10 × 250 mm) using acetonitrile (solvent A) and 30 mM ammonium acetate (solvent B) as the mobile phases (gradient: solvent A was increased from 5% to 25% over 25 min; 3.5 mL/min). Following removal of the DMT group by incubation in 80% glacial acetic acid for 12 min at room temperature the oligonucleotides were subjected to a second round of HPLC purification (gradient: solvent A was increased from 0% to 15% over 35 min; 3.5 mL/min).

Optical Melting Analysis. Quantification of oligonucleotides was performed at 90 °C using the ε_{260} values estimated for single-stranded DNA (*13*) and a Beckman Coulter DU800 UV−vis equipped with a Peltier thermoelectric device. Optical melting analysis was performed using DNA concentrations ranging from 0.2 to 2.0 μM in 50 mM sodium phosphate, 25 mM $NaHCO_3$, and 10 mM NaCl, pH 7.5. Prior to analysis samples were incubated for 5 min at 90 °C and cooled to room temperature over ~2.5 h. The samples were then heated at a rate of 1 °C/min from 25 to 90 °C while monitoring absorbance at 260 nm, held at 90 °C for 5 min, followed by cooling at a rate of 1 °C/min to return to the starting temperature. The first derivative of the absorbance versus temperature data was obtained and the T_m taken as the maximum in the first derivative plot.

Chemical Probe Analysis and Peroxynitrite Reactions. Peroxynitrite (Cayman Chemical) was aliquoted, stored at −80 °C, quantified by UV−vis using $\varepsilon_{302} = 1670\ M^{-1}\ cm^{-1}$ prior to each use, and diluted as necessary using cold 0.3 M NaOH.

Oligonucleotides were 5′-^{32}P end-labeled following the manufacturer's protocol. To obtain the duplex and hairpin assemblies (5 μM), the appropriate oligonucleotides, in 50 mM sodium phosphate, 25 mM $NaHCO_3$, and 10 mM NaCl, pH 7.5, were incubated for 5 min at 90 °C and cooled over ~2.5 h to room temperature. Since the chemistry of peroxynitrite is modulated by CO_2 (*14*, *15*), all experiments were conducted in the presence of 25 mM $NaHCO_3$ to maintain the concentration of CO_2 in the buffer at ~1 mM, which is comparable to physiological levels. The DNA assemblies were incubated with varying concentrations of DEPC for 30 min at room temperature or with $ONOO^-$ for 30 min at 37 °C. Following incubation with DEPC or $ONOO^-$ the samples were dried *in vacuo*, treated with 10% piperidine (v/v) for 30 min at 90 °C, and again dried *in vacuo*. Samples were resuspended in denaturing loading buffer (80% formamide, 0.1% xylene cyanol, 0.1% bromphenol blue), incubated for 3 min at 90 °C, and electrophoresed through a 18% denaturing polyacrylamide gel. The products were visualized by phosphorimagery.

Expression and Purification of hOGG1. *Escherichia coli* BL21(DE3)pLysS cells were transformed via heat shock with the hOGG1 pET30a plasmid (*16*) (a generous gift of the Verdine laboratory) that encodes for the wild-type enzyme with an N-terminal His_6 tag. The transformed cells were grown to an OD_{600} = 0.5−0.6 at 37 °C in 4 L of LB media (containing 34 μg/mL kanamycin and 34 μg/mL chloramphenicol), cooled to 30 °C, and induced using 1 mM IPTG. After 3 h of growth at 30 °C the cells were pelleted by centrifugation (5000 rpm, 30 min, 4 °C). The supernatant was discarded, and the cells were frozen with liquid nitrogen and stored at −80 °C until purification. Upon thawing the cells were suspended in 35 mL of 20 mM Tris-HCl, 20% glycerol, 5 mM imidazole, and 500 mM KCl, pH 7.5, supplemented with 1 mM PMSF and 100 μL of 2 mg/mL pepstatin A/leupeptin, and lysis was performed using a French press. Lysates were clarified by centrifugation (13000 rpm, 90 min, 4 °C), and supernatant was loaded onto a 10 mL Ni-NTA resin (Qiagen) column and washed with 50 mL of 20 mM Tris-HCl, 20% glycerol, and 500 mM KCl, pH 7.5 (buffer X), supplemented with 5 mM imidazole. The column was then washed with 50 mL of buffer X supplemented with 20 mM imidazole, followed by 50 mL of buffer X supplemented with 500 mM imidazole to elute the protein containing the His_6 tag. Protein was concentrated using an Amicon ultrafiltration cell and suspended in storage buffer (20 mM Tris-HCl, 100 mM KCl, 10 mM 2-mercaptoethanol, 50% glycerol, pH 7.5), frozen with liquid nitrogen in 200 μL aliquots, and stored at −80 °C. SDS−PAGE and Coomassie stain analysis show the protein to be >90% pure. The N-terminal His_6 tag was not removed prior to kinetic analysis, as analysis of hOGG1 lacking the His_6 tag has previously been shown to demonstrate no difference in single-turnover rate constants (*17*).

Active Site Titration. The total concentration of hOGG1 was determined by the Bradford method using bovine γ-globulin as a standard. In order to determine the concentration of active enzyme, an active site titration was performed as previously described (*18*) using the mixed-sequence 8-oxoG-containing duplex (Supporting Information). The DNA substrate in 20 mM Tris-HCl, 10 mM Na_2EDTA, and 140 nM NaCl, pH 7.6, was annealed by incubating the 8-oxoG-containing oligonucleotide with a 1.25-fold excess of the complementary oligonucleotide for 5 min at 90 °C followed by cooling over ~2.5 h to room temperature. Analysis by native PAGE confirmed the formation of duplex and, importantly, the absence of single-stranded ^{32}P-labeled DNA. The annealed DNA substrate was diluted using 20 mM Tris-HCl, 10 mM Na_2EDTA, and 240 μg/mL BSA, pH 7.6, to yield a final DNA concentration of 20 nM in 20 mM Tris-HCl, 10 mM Na_2EDTA, 80 mM NaCl, and 100 μg/mL BSA, pH 7.6. Prior to addition of hOGG1 the DNA samples were equilibrated for 5 min at 37 °C. The hOGG1 enzyme was diluted as necessary in 20 mM Tris-HCl, 10 mM Na_2EDTA, and 100 μg/mL BSA, pH 7.6, and stored on ice prior to use. For the

active site titration the concentration of hOGG1 was adjusted to provide less than 15% conversion to product in order to preserve multiple-turnover conditions (*18*). Following addition of hOGG1, the 60 μL sample was incubated at 37 °C, and aliquots (5 μL) were removed as a function of time, quenched by the addition of 5 μL of 0.5 M NaOH, and incubated for 2 min at 90 °C. Quenching with NaOH/heat ensures that the β-lyase activity of hOGG1 is not limiting the observed rates of reactions (*17*, *19*). Following quenching with NaOH/heat, denaturing loading buffer (5 μL) was added, and the samples were kept on dry ice until electrophoresis. To analyze the products of the reaction, the samples were removed from dry ice, heat denatured for 3 min at 90 °C, and electrophoresed through an 18% denaturing polyacrylamide gel. The products were visualized by phosphorimagery. The concentration of product as a function of time was plotted and the amount of active enzyme determined to be 43% by extrapolating the linear portion of the plot to the *y*-intercept (*18*). All hOGG1 concentrations given below or in figure captions are active enzyme concentrations.

Glycosylase Activity Assay. These experiments were conducted using 20 nM DNA substrate and the same reaction conditions and protocol as the active site titration except, notably, the enzyme concentration was 100 nM. This enzyme concentration ensures single-turnover conditions for hOGG1 (*17*). In addition to performing experiments in which the reaction was quenched by the addition of NaOH/heat, single-turnover experiments were also performed without NaOH/heat treatment. In these cases, denaturing loading buffer (5 μL) was added to the samples, which were then kept on dry ice until electrophoresis. The products were visualized by phosphorimagery, and KaleidaGraph was used to fit the data as previously described (*17*) to obtain the rate of substrate to product conversion (k_2).

RESULTS

Design and Characterization of DNA Assemblies. Two DNA assemblies were designed for these studies (Figure 1). The first assembly is a double-stranded $(CAG)_{10}/(CTG)_{10}$ duplex which is comprised entirely of Watson−Crick G·C and A·T base pairs. The second assembly is a $(CAG)_{10}$ hairpin which consists of a loop and stem region; the hairpin stem contains both G·C base pairs and A·A mismatches. In addition, as an internal control for susceptibility to damage, both assemblies contain 10 base pairs of mixed-sequence duplex.

The assemblies were characterized first using optical melting analysis. The $(CAG)_{10}/(CTG)_{10}$ duplex and $(CAG)_{10}$ hairpin assemblies each display a single, sharp transition in the absorbance profile which defines melting temperatures (T_m) of 80.5 and 70.7 °C, respectively (Supporting Information). Importantly, the T_m of the $(CAG)_{10}$ hairpin does not vary over a 10-fold range in concentration which is consistent with the formation of an intramolecular structure (*20*). Furthermore, as expected for duplex and hairpin structures, little or no hysteresis between the melting and annealing curves is observed.

In addition to optical melting analysis the DNA assemblies were also characterized based on their modification by diethyl pyrocarbonate (DEPC), a chemical probe of nucleobase accessibility (Figure 2). DEPC selectively modifies unpaired purines (A ≫ G) and has been used previously to identify nucleobases in hairpin loops and DNA bulges (*7*, *21*). Hyperreactivity of two adenines and one guanine in the $(CAG)_{10}$ hairpin allows us to define the hairpin loop as the four nucleobases shown in Figure 2.

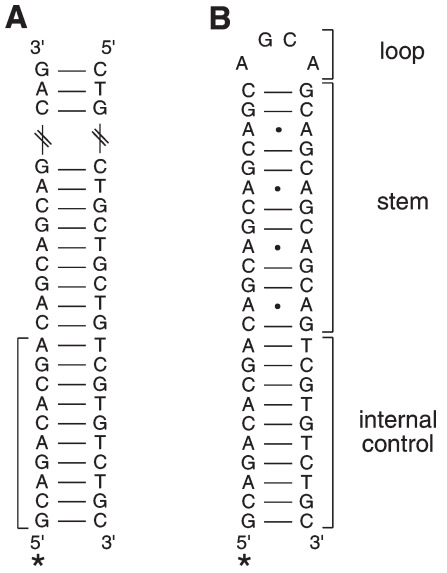

FIGURE 1: Schematic illustration of (A) the $(CAG)_{10}/(CTG)_{10}$ duplex and (B) $(CAG)_{10}$ hairpin assemblies utilized in this work. The asterisk represents the location of the ^{32}P-radiolabel.

The adenines in the stem of the hairpin are also modified by DEPC, although to a lesser extent than those in the loop; this reactivity is consistent with increased dynamics at A·A mismatch sites. As expected for well-matched Watson−Crick base pairs, the adenines and guanines in the duplex assembly as well as in the mixed-sequence internal control regions of the duplex and hairpin assemblies are not modified by DEPC.

To examine the ability of the internal control region to modulate the structure adopted by the repetitive DNA, the $(CAG)_{10}/(CTG)_{10}$ duplex and $(CAG)_{10}$ hairpin assemblies were also prepared without the 10 base pairs of mixed sequence. Based on optical melting analysis the duplex and hairpin assemblies form as expected (Supporting Information). Inclusion of this internal control, however, may minimize the conformational space sampled by the hairpin assembly leading to sharper optical melting transitions (*22*).

Modification of the $(CAG)_{10}/(CTG)_{10}$ Duplex and $(CAG)_{10}$ Hairpin Assemblies by Peroxynitrite. To determine the susceptibility of the $(CAG)_{10}/(CTG)_{10}$ duplex and $(CAG)_{10}$ hairpin to DNA damage, the two assemblies were incubated with peroxynitrite ($ONOO^-$), a powerful oxidizing and nitrating agent generated as part of the immune response. Of the four DNA nucleobases G has the lowest redox potential (*23*) and is selectively modified by peroxynitrite (*24*). Indeed, upon exposure to peroxynitrite G is converted to three major products, 8-oxoG, 8-nitroguanine, and 5-guanidino-4-nitroimidazole (*24*). Under our experimental conditions 8-nitroguanine depurinates and will be converted to a strand break upon piperidine treatment (*25*). Additionally, DNA containing 5-guanidino-4-nitroimidazole is partially converted to a strand break upon piperidine treatment (*26*). It is noteworthy that 8-oxoG is refractory to cleavage by piperidine (*27*), and therefore, if strand cleavage is observed at a given G, it likely represents an underestimate of the total amount of damage.

For both the duplex and hairpin assemblies there is no strand cleavage observed in the absence of peroxynitrite (Figure 3). Furthermore, in the presence of peroxynitrite no significant strand cleavage is observed in the $(CAG)_{10}/(CTG)_{10}$ duplex assembly. The absence of strand cleavage indicates that the

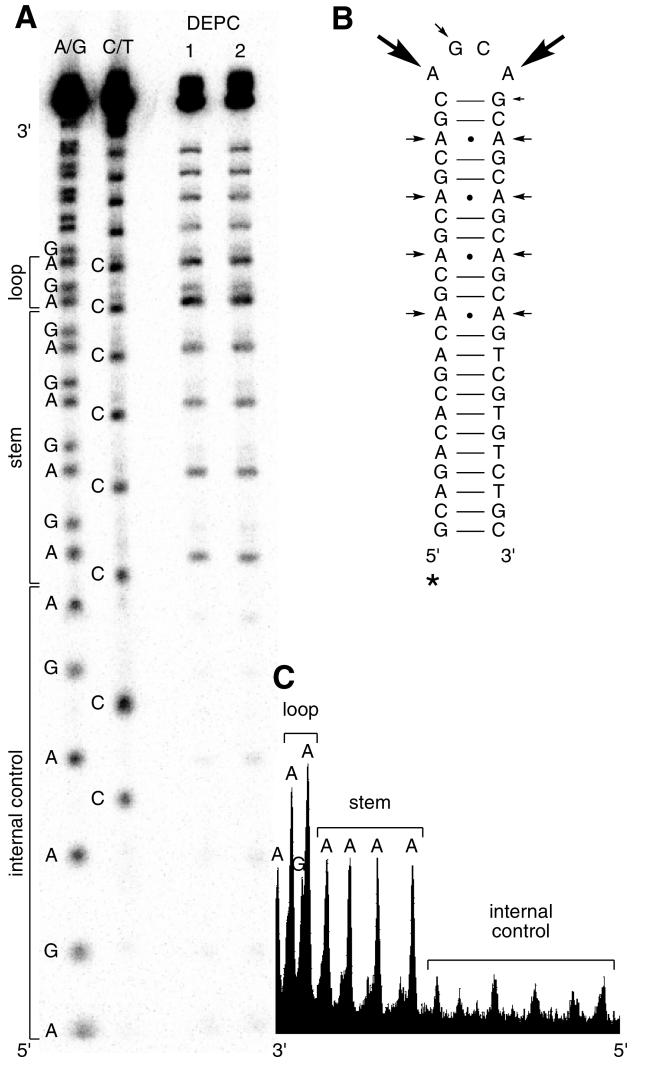

FIGURE 2: Characterization of the $(CAG)_{10}$ hairpin assembly using the chemical probe DEPC. (A) Autoradiogram revealing strand cleavage of $(CAG)_{10}$ hairpin assembly (5 μM) in 50 mM sodium phosphate, 25 mM $NaHCO_3$, and 10 mM NaCl, pH 7.5, by DEPC (69 mM and 138 mM in lanes 1 and 2, respectively) following incubation for 30 min at 37 °C and piperidine treatment. A/G and C/T are Maxam−Gilbert sequencing reactions. (B) Schematic representation of the location of damage induced by DEPC. The size of the arrow at a given site reflects the relative amount of strand cleavage. The asterisk represents the location of the ^{32}P-radiolabel. (C) Histogram representing strand cleavage in lane 2 of panel A, revealing hyperreactivity of two adenines and one guanine in the $(CAG)_{10}$ hairpin assembly.

duplex assembly is not readily susceptible to modification by peroxynitrite under these conditions. In addition, no strand cleavage is observed in the internal control region of the duplex assembly. In contrast to these results with the duplex assembly, strand cleavage is observed in the $(CAG)_{10}$ hairpin after exposure to peroxynitrite. In fact, in a concentration-dependent manner, peroxynitrite selectively modifies a single G in the hairpin assembly. This G is unique in that it is in the loop region of the hairpin. Importantly, similar to the internal control region of the $(CAG)_{10}/(CTG)_{10}$ duplex assembly no strand cleavage is observed in the internal control region of the $(CAG)_{10}$ hairpin assembly. This lack of reactivity in the internal control regions allows us to make direct comparisons between the amount of modification by peroxynitrite of the $(CAG)_{10}$ sequence in the context of a hairpin versus duplex. Indeed, we find that, under the same reaction conditions, when present in the context of a duplex the $(CAG)_{10}$ sequence is protected from modification by peroxynitrite, but this same sequence is susceptible to peroxynitrite when in a hairpin conformation. Furthermore, for the $(CAG)_{10}$ hairpin the G in the loop represents a hot spot for DNA damage.

We next examined if the susceptibility to peroxynitrite is a general phenomenon dependent on the hairpin structure, rather than purely a consequence of the $(CAG)_{10}$ sequence. To accomplish this, a hairpin assembly was constructed using a nonrepetitive sequence (Supporting Information). Based on its reactivity toward DEPC, this nonrepetitive sequence hairpin contains a single G in a four nucleobase loop. However, in contrast to the $(CAG)_{10}$ hairpin, the hairpin stem is comprised of a mixed sequence of G·C and A·T Watson−Crick base pairs. We find that peroxynitrite selectively modifies the G in the loop region, confirming that the reactivity is derived from structure and not sequence (Supporting Information).

Glycosylase Activity of Human OGG1 with the 8-OxoG-Containing Duplex and Hairpin Substrates. Having demonstrated a structure-dependent susceptibility of the $(CAG)_{10}$ sequence to peroxynitrite, we next examined the ability of hOGG1 to remove DNA damage from assemblies containing the repetitive sequence. In order to obtain a homogeneous substrate for these repair studies, we did not use the products of the peroxynitrite reactions directly, but rather chemically synthesized DNA containing a site-specific 8-oxoG.

Five DNA substrates were utilized in these repair studies; in each case the 8-oxoG-containing strand was 5′-^{32}P end-labeled (Figure 4). The first substrate is a $(CAG)_{10}$ hairpin in which the G in the loop, the G that is selectively modified by peroxynitrite, is replaced by 8-oxoG (loop-HP). The ability of hOGG1 to remove 8-oxoG from this substrate is of particular interest given the propensity for damage to form at this site. In the second substrate, this 8-oxoG-containing strand is base paired to $(CTG)_{10}$ to yield a duplex (loop-DUP). The third substrate is a $(CAG)_{10}$ hairpin in which 8-oxoG replaces a G in the stem (stem-HP). In the fourth substrate, this 8-oxoG-containing strand is base paired to $(CTG)_{10}$ to generate a duplex (stem-DUP). Importantly, chemical probe analysis with DEPC showed that, similar to sequences lacking 8-oxoG, substrates containing 8-oxoG in the stem or loop form hairpins with loops containing four nucleobases (Supporting Information). Furthermore, we find that unpaired 8-oxoG is modified by DEPC to an extent similar to unpaired A. The final substrate is a 30 base pair mixed-sequence duplex containing 8-oxoG (mixed-DUP). Although we did not observe peroxynitrite-induced damage in the hairpin stem or duplex, we used substrates 2−4 as controls for hOGG1 activity on the repetitive sequence. The mixed-sequence duplex serves as a reference for enzyme activity since this substrate has been used previously to establish kinetic parameters for hOGG1 (*19*).

With most glycosylases product release is rate limiting (*28*). Therefore, k_{cat} measured under steady-state conditions is primarily a reflection of the rate of product release rather than the glycosylase step. By carrying out experiments under single-turnover conditions ([hOGG1] ≫ [DNA]) the intrinsic properties of 8-oxoG removal are revealed because complications associated with product release are eliminated. In addition to catalyzing removal of 8-oxoG, hOGG1 also possesses β-lyase activity which converts the AP site to a strand break 3′ to the original 8-oxoG site (*11*). When the reaction is quenched by freezing on dry ice, k_{obs} includes the glycosylase and β-lyase reactions. In fact, it has been shown previously that in the absence of NaOH/heat

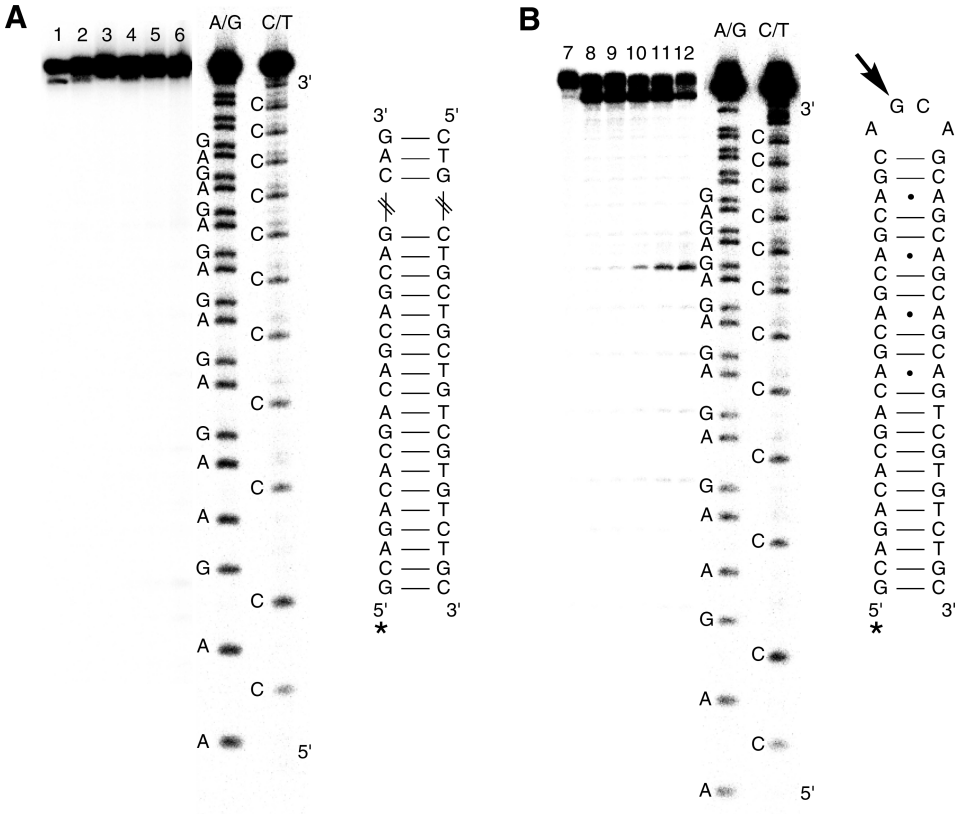

FIGURE 3: Susceptibility of DNA assemblies to modification by peroxynitrite. Autoradiogram revealing strand cleavage of (A) the $(CAG)_{10}/(CTG)_{10}$ duplex assembly and (B) the $(CAG)_{10}$ hairpin assembly following exposure to peroxynitrite. Conditions are 5 μM DNA in 50 mM sodium phosphate, 25 mM $NaHCO_3$, and 10 mM NaCl, pH 7.5. Lanes 1 and 2 and lanes 7 and 8 contain DNA alone and piperidine-treated DNA, respectively. Lanes 3−6 and 9−12 contain DNA incubated for 30 min at 37 °C in the presence of an increasing concentration of peroxynitrite (0, 100, 1000, and 2500 μM, respectively) followed by piperidine treatment. A/G and C/T are Maxam−Gilbert sequencing reactions. The arrow indicates site of modification by peroxynitrite. The asterisk represents the location of the ^{32}P-radiolabel.

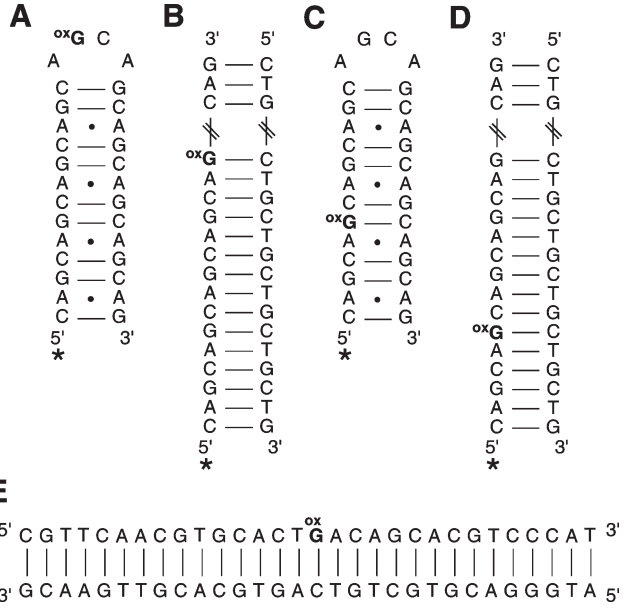

FIGURE 4: Schematic illustration of the assemblies used in the hOGG1 glycosylase reactions: (A) $(CAG)_{10}$ hairpin with 8-oxoG in the loop (loop-HP), (B) duplex obtained by base pairing loop-HP to $(CTG)_{10}$ (loop-DUP), (C) $(CAG)_{10}$ hairpin with 8-oxoG in the stem (stem-HP), (D) duplex obtained by base pairing stem-HP to $(CTG)_{10}$ (stem-DUP), and (E) mixed-sequence duplex (mixed-DUP). The asterisk represents the location of the ^{32}P-radiolabel.

treatment k_{obs} reflects the rate constant for the β-lyase step (*19*). The use of NaOH/heat treatment ensures that the β-lyase step does not limit the observed rate, and therefore, k_{obs} reflects the rate constant for the glycosylase step (*17*, *19*).

The rate constant k_2 was first determined using NaOH/heat treatment to quench the reaction. As previously demonstrated, the rate of reaction of hOGG1 with mixed-DUP is too fast to measure accurately by manual methods (Supporting Information) (*19*). Nevertheless, since the first time point assayed (15 s) corresponds to ~85% product, which is approximately three half-lives, an upper limit for the half-life of ≤5 s and thus a lower limit for $k_2 \geq 8$ min^{-1} could be estimated (*18*). Indeed, using a rapid quench instrument the rate constant k_2 for removal of 8-oxoG from mixed-DUP was previously reported as 50 ± 7 min^{-1} (*19*). In addition to mixed-DUP, we find that the rate of removal of 8-oxoG from loop-DUP is also too fast to measure by manual methods. Based on the observation that the first time point assayed (15 s) corresponds to ~75% product, a lower limit for $k_2 \geq 6$ min^{-1} could be estimated (*18*).

Under the same reaction conditions, however, k_2 could be measured using manual methods for stem-DUP, stem-HP, and loop-HP. As seen in Figure 5, the product of the glycosylase reaction accumulates as a function of time for stem-HP (Figure 5A). For loop-HP, the hairpin substrate containing 8-oxoG in the loop, product also accumulates as a function of time although more slowly than for stem-HP. As described previously (*18*), these data were fitted with the appropriate rate equation to extract the rate constant for the substrate to product conversion (k_2) (Figure 6). When NaOH/heat was used to quench the reaction, the rate constant k_2 for removal of 8-oxoG by hOGG1 from stem-DUP, stem-HP, and loop-HP is slower than

that observed for removal of 8-oxoG from mixed-DUP and loop-DUP (Table 1). Using the reported k_2 value of 50 ± 7 min^{-1} for mixed-DUP (*19*), the hOGG1 enzyme removes 8-oxoG from stem-DUP and stem-HP with rate constants ~17 and ~38 times slower, respectively, than from the mixed-sequence duplex. Furthermore, the reaction of hOGG1 with the hairpin containing 8-oxoG in the loop is ~700 times slower than with mixed-DUP.

The rate constant k_2 was also determined without NaOH/heat treatment. Under these conditions rate constants could be determined, using manual methods, for all five DNA substrates. For mixed-DUP, k_2 is markedly slower in the absence of NaOH/heat treatment (Table 1) (Supporting Information) (*19*). Additionally, the rate of removal of 8-oxoG from loop-DUP, stem-DUP, and stem-HP is also slower in the absence of NaOH/heat treatment (Figure 7). In contrast, however, k_2 was found to be 0.07 ± 0.004 for loop-HP in both the absence and presence of NaOH/treatment; no difference was observed in the measured rate constant for this hairpin substrate upon NaOH/heat treatment. Interestingly, whereas the same overall product yield was observed for the duplex substrates in the absence and presence of NaOH/heat treatment, the overall product yield for both hairpin substrates, stem-HP and loop-HP, is reduced 2- and 4-fold, respectively, in the absence of NaOH/heat treatment.

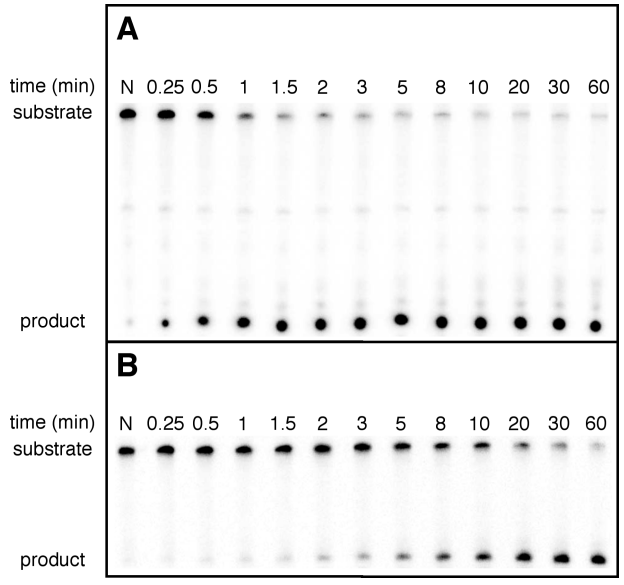

FIGURE 5: Removal of 8-oxoG from hairpin substrates by hOGG1. Autoradiogram revealing strand cleavage upon treatment of (A) stem-HP and (B) loop-HP with hOGG1 followed by NaOH/heat treatment. Reaction conditions are 20 nM DNA and 100 nM hOGG1 in 20 mM Tris-HCl, 10 mM Na_2EDTA, 80 nM NaCl, and 100 μg/mL BSA, pH 7.6. Samples were incubated for 0.25−60 min at 37 °C, followed by NaOH/heat treatment. N represents DNA alone with no hOGG1.

DISCUSSION

We have demonstrated the structure-dependent modification of a trinucleotide repeat sequence. Peroxynitrite provides a suitable reactive species as it is generated biologically and, furthermore, one of the products of G modification is 8-oxoG, which represents the prototypic substrate for hOGG1. Our results suggest that $(CAG)_n$ sequences within the duplex are protected from solution-borne species, but if these same sequences adopt

Table 1: Rate Constants for the Removal of 8-OxoG by hOGG1 with Duplex and Hairpin Substrates

	k_2 (min^{-1})[a]	
substrate	+NaOH/heat	−NaOH/heat
mixed-DUP	≥8	1.6 ± 0.11
loop-DUP	≥6	1.1 ± 0.05
stem-DUP	2.8 ± 0.17	0.59 ± 0.06
stem-HP	1.3 ± 0.11	0.06 ± 0.006
loop-HP	0.07 ± 0.004	0.07 ± 0.004

[a] Rate constants (k_2) for hOGG1 measured at 37 °C under single-turnover conditions. All values represent results from a single experiment, and error represents the standard deviation associated with data fit. Multiple experiments were performed, and the results were the same within experimental error.

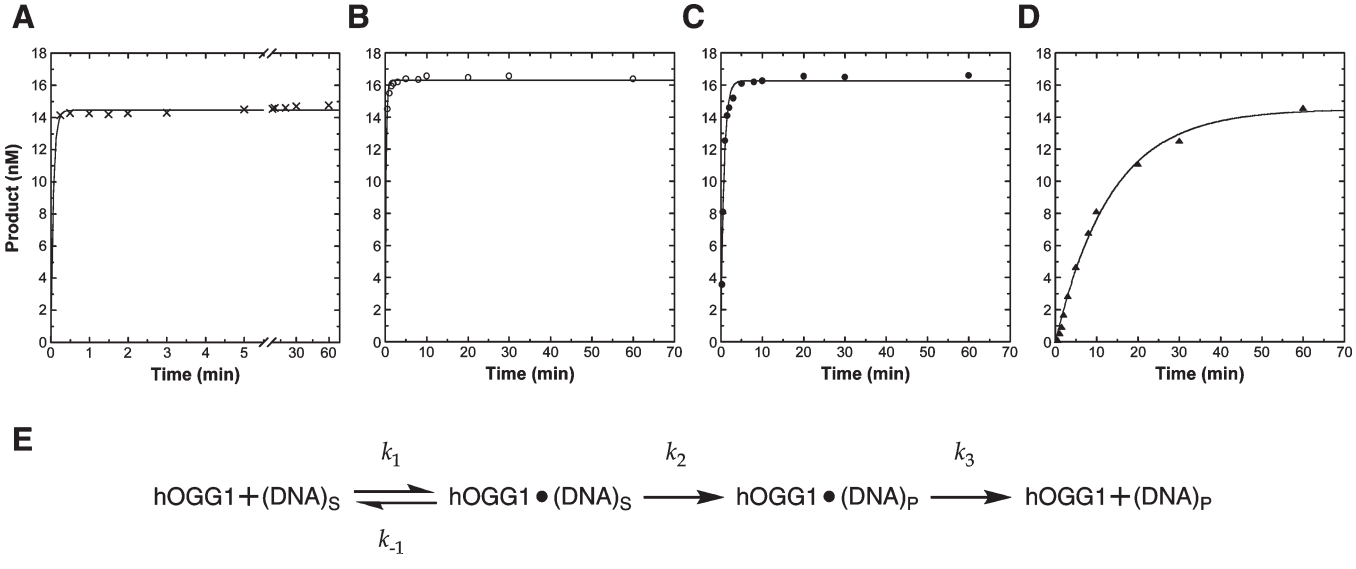

FIGURE 6: Graphical representation of time course data for removal of 8-oxoG by hOGG1 from (A) loop-DUP, (B) stem-DUP, (C) stem-HP, and (D) loop-HP following NaOH/heat treatment. Reaction conditions are 20 nM DNA and 100 nM hOGG1 in 20 mM Tris-HCl, 10 mM Na_2EDTA, 80 nM NaCl, and 100 μg/mL BSA, pH 7.6. Samples were incubated for 0.25−60 min at 37 °C, followed by NaOH/heat treatment. The data are fitted to a single exponential to determine the rate constant k_2. (E) Minimal kinetic scheme used for analysis of hOGG1 glycosylase activity, where S and P indicate DNA substrate and product, respectively.

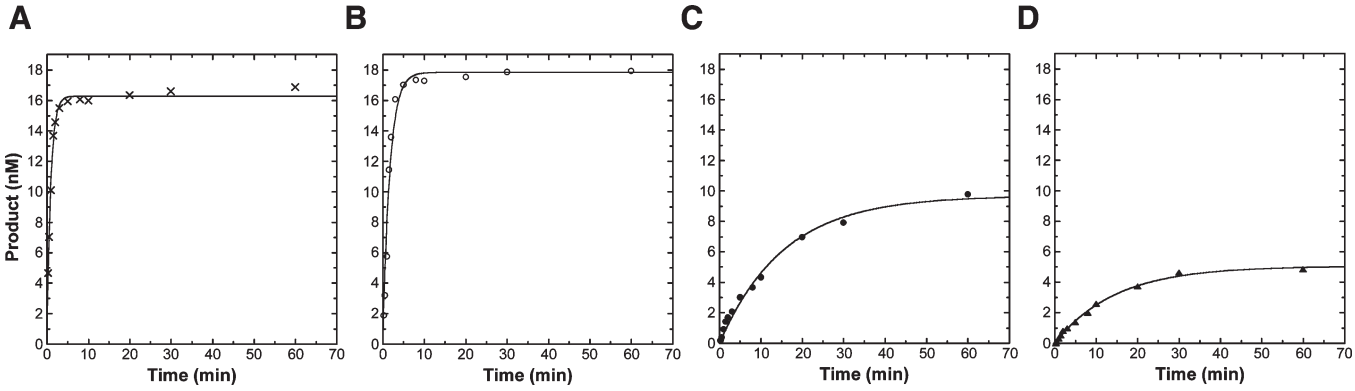

FIGURE 7: Graphical representation of time course data for removal of 8-oxoG by hOGG1 from (A) loop-DUP, (B) stem-DUP, (C) stem-HP, and (D) loop-HP in the absence of NaOH/heat treatment. Reaction conditions are 20 nM DNA and 100 nM hOGG1 in 20 mM Tris-HCl, 10 mM Na_2EDTA, 80 nM NaCl, and 100 μg/mL BSA, pH 7.6. Samples were incubated for 0.25−60 min at 37 °C. The data are fitted to a single exponential to determine the rate constant k_2.

a hairpin conformation, they are susceptible to modification. Interestingly, the increased dynamics of the A·A mismatches in the hairpin stem, as observed by their reactivity toward DEPC, does not render the adjacent guanines susceptible to peroxynitrite. Only the G in the loop of the $(CAG)_{10}$ hairpin is a hot spot for damage.

Furthermore, we have shown that susceptibility of G to peroxynitrite is a general phenomenon dependent on the hairpin structure, rather than purely a consequence of the $(CAG)_{10}$ sequence. Indeed, peroxynitrite selectively modifies the G in the loop region of the mixed-sequence hairpin. It is noteworthy, however, particularly in the case of the repetitive $(CAG)_n$ trinucleotide motif that the sequence is what dictates hairpin formation. Thus, while we examined damage patterns in the $(CAG)_{10}$ hairpin, we would also expect that if a hairpin were to form from the complementary CTG strand, any unpaired guanines would also be susceptible to peroxynitrite.

This reactivity of peroxynitrite at unpaired nucleobases is consistent with literature reports in which chemical probes of nucleobase accessibility preferentially modify nucleobases in hairpin loops and bulges (*7*, *21*, *29*, *30*). Furthermore, it has been shown previously that an oxoruthenium(IV) complex preferentially oxidizes guanines in the loop of a hairpin over guanines in the stem (*31*). In addition, consistent with the results obtained in this work, the amount of G oxidation by the oxoruthenium(IV) complex in the hairpin loop was dramatically reduced when the sequence was base paired to the complementary strand to form a duplex substrate (*31*). Additionally, increased dynamics in the loop of a CAG repeat hairpin, relative to the stem region, has been demonstrated using the fluorescent nucleobase analogue 2-aminopurine (*32*). Taken together, these data suggest that the susceptibility to peroxynitrite of the G in the loop of the $(CAG)_{10}$ hairpin is due to increased solution accessibility relative to the guanines in the stem of the hairpin or in $(CAG)_{10}/(CTG)_{10}$ duplex. All of the other guanines in the hairpin or duplex substrate are base paired to C and are well stacked in the stem or duplex and, therefore, protected from modification by peroxynitrite.

With respect to repair by hOGG1, previous work has shown that hOGG1 can, in fact, excise 8-oxoG from duplex containing a repetitive CAG/CTG sequence. McMurray and co-workers reconstituted the hOGG1-initiated BER repair event *in vitro* using two 100 base pair duplex substrates; each duplex contained a single 8-oxoG flanked either by mixed sequence or by mixed sequence to the 5′-side and $(CAG)_{19}/(CTG)_{19}$ to the 3′-side (*9*). Using purified hOGG1, 8-oxoG was excised from both duplexes although kinetic parameters were not reported. Furthermore, APE1 also had similar activity on both duplexes; following removal of 8-oxoG by hOGG1 to generate an AP site, addition of APE1 resulted in nicking of the phosphodiester backbone of both substrates (*9*). In contrast to hOGG1 and APE1, which had similar activity on both DNA substrates, pol β faithfully completed gap-filling synthesis on the mixed-sequence duplex, but longer addition products were obtained for the duplex containing $(CAG)_{19}/(CTG)_{19}$ (*9*). Following ligation, a 100 base pair product was restored for the mixed-sequence duplex, but expanded products were obtained for the duplex containing the repeat sequence. Thus, hOGG1 can mediate expansion during the gap-filling step of BER.

Our results with $(CAG)_{10}/(CTG)_{10}$ duplexes containing a site-specific 8-oxoG are consistent with this previously reported work. We find that hOGG1 removes 8-oxoG from duplexes comprised solely of CAG/CTG repeats, and our experiments have established lower limits of k_2 for loop-DUP and mixed-DUP of $k_2 \geq 6$ and 8 min^{-1}, respectively. Indeed, a k_2 of 50 ± 7 min^{-1} has previously been reported for mixed-DUP (*19*). Experiments would need to be performed using a rapid quench apparatus to obtain k_2 for loop-DUP and determine if the repetitive sequence suppresses the glycosylase activity of hOGG1. Nevertheless, we have shown that removal of 8-oxoG from loop-DUP is faster than from the other trinucleotide repeat substrates.

For instance, in contrast to loop-DUP, quantitative data for k_2 could be obtained using manual methods for stem-DUP; k_2 was found to be 2.8 ± 0.17 min^{-1}. While both of these duplex substrates, loop-DUP and stem-DUP, are comprised of the $(CAG)_{10}/(CTG)_{10}$ sequence, the 8-oxoG is in different locations. For loop-DUP the 8-oxoG is located in the center of the 30-mer duplex; for stem-DUP the 8-oxoG is 5 base pairs from the end of the duplex. Indeed, previous work has shown that the location of the 8-oxoG with respect to the end of the duplex can influence OGG1 activity (*17*, *19*). A slower k_2 was observed when the 8-oxoG was located 9 base pairs from the end of the duplex as compared to when the 8-oxoG was in the center of a 30-mer duplex (*17*).

In addition to removing 8-oxoG from the repeat-sequence duplexes we find that hOGG1 also removes 8-oxoG from the hairpin substrates, albeit with decreased efficiency. The rate of removal of 8-oxoG from stem-HP is ~2 times slower than that

observed for the corresponding duplex substrate stem-DUP. For the hairpin substrate containing 8-oxoG in the loop we find that hOGG1 removes 8-oxoG with a rate ~700 times slower than mixed-DUP; this estimate is obtained using the previously reported k_2 of 50 ± 7 min^{-1} for mixed-DUP. Therefore, our results have shown that the unpaired G in the hairpin loop is most susceptible to DNA damage, yet this site is repaired least efficiently by hOGG1.

Indeed, while the hOGG1 enzyme is able to remove 8-oxoG from both the stem and loop of a hairpin, the enzyme is ~18 times more efficient at removing 8-oxoG from the stem, which structurally resembles duplex, than from the hairpin loop, which is more single stranded in nature. Interestingly, previous work has shown that hOGG1 cannot remove 8-oxoG from unstructured single-stranded DNA or from an 11 nucleobase loop (*33*). It is noteworthy that although the efficiency is reduced, hOGG1 is able to remove 8-oxoG from the loop of the $(CAG)_{10}$ hairpin. This indicates that hOGG1 does recognize and bind to the loop of the hairpin. This also suggests that the four nucleobase loop of the $(CAG)_{10}$ hairpin, as opposed to a purely single-stranded region or an 11 nucleobase loop, provides a structure which is sufficient for hOGG1 recognition and binding.

Examination of a hOGG1/DNA duplex cocrystal structure obtained with a recognition-competent but catalytically inactive hOGG1 mutant revealed that the 8-oxoG is flipped out of the DNA helix and into the active site of the enzyme (*34*). The enzyme participates in hydrogen bonding to both the Watson−Crick face of 8-oxoG and the N7−H. In addition to these interactions with the 8-oxoG, hOGG1 makes extensive contacts with the estranged C. With respect to the lower efficiency of hOGG1 on the hairpin containing 8-oxoG in the loop, while the 8-oxoG is available for enzyme binding and, in fact, the single-stranded nature of the loop could facilitate its extrusion from the DNA, the estranged C is not present. However, it is possible that when bound by hOGG1 a base from the hairpin loop or stem may occupy the site of the estranged C.

Single-turnover experiments were also performed without NaOH/heat treatment; under these conditions the β-lyase activity of hOGG1 provides strand scission. Kinetic parameters for the same mixed-sequence duplex utilized in this work, mixed-DUP, have previously been reported; the β-lyase activity of hOGG1was found to be decoupled from the glycosylase activity (*19*). We find that the observed rate of 8-oxoG removal is indeed faster for mixed-DUP, loop-DUP, stem-DUP, and stem-HP when NaOH/heat is used to quench the reaction. Thus, for these DNA substrates the glycosylase and β-lyase activities of hOGG1 are decoupled. Interestingly, however, for loop-HP no difference in k_2 was observed when NaOH/heat was used to quench the reaction. It is also of note that in the absence of NaOH/heat treatment the overall product yield for stem-HP and loop-HP is reduced relative to when NaOH/heat treatment is used. With NaOH/heat treatment the yield of product was ~80% for both hairpin substrates. However, in the absence of NaOH/heat treatment the overall product yield was 50% and 25% for stem-HP and loop-HP, respectively. These data show that the β-lyase activity of hOGG1 is less efficient on the hairpin as opposed to duplex substrates. Treatment with NaOH/heat is required to convert all AP sites within the hairpin to product.

The observation of structure-dependent damage and repair patterns in the CAG/CTG repeat sequence may be significant with respect to the OGG1-dependent trinucleotide repeat expansion observed in mouse models of HD (*9*). The formation of non-B DNA conformations, such as hairpins, has been proposed to play a key role in repeat expansion (*4*, *5*). Here we show that the formation of non-B conformations renders the DNA more susceptible to solution-borne reactive species yet also decreases the efficiency of repair by hOGG1. Although the efficiency of removal of 8-oxoG from the loop is reduced relative to duplex, repeat expansion may still be initiated on a hairpin substrate if the downstream BER events, in particular the pol β-catalyzed gap-filling step, are not faithfully completed.

As an alternative to a repair-dependent expansion mechanism, hOGG1 may also contribute to a replication-dependent trinucleotide repeat expansion. Although its catalytic activity is reduced, hOGG1 clearly recognizes and binds to the hairpin substrate containing 8-oxoG in the loop. Indeed, binding to the damage-containing non-B conformation may further stabilize the structure, allowing it to persist. The stabilized non-B conformation could then be replicated by DNA polymerase with the full length of the hairpin being incorporated into the nascent strand. This would result in a replication-dependent expansion. Indeed, there is precedence for protein stabilization of non-B conformations; the human Ku antigen was found previously to bind a trinucleotide repeat hairpin with a K_d of 9.6 nM (*35*).

Furthermore, there is also precedence for binding to a trinucleotide repeat hairpin to inhibit or decrease enzyme activity as we observed for hOGG1. *In vitro* analysis of an Msh2/Msh3−$(CAG)_n$ hairpin complex revealed that binding to the $(CAG)_n$ hairpin suppresses most of the protein functions required for removal of single-base insertions and small extrahelical loops (*36*). The ability of hOGG1 and a damage-containing hairpin to modulate replication-dependent trinucleotide repeat expansion will be explored as part of our future studies along with the ability of pol β to complete gap-filling on the hairpin substrate.

In conclusion, we have found that a hairpin conformation adopted by a trinucleotide repeat sequence is more susceptible to damage than the corresponding DNA duplex. In particular, the unpaired G in the loop of the hairpin represents a hot spot for damage. This particular hot spot for damage is also inefficiently repaired by hOGG1. These structure-dependent patterns of DNA damage and repair observed for a trinucleotide repeat sequence may have implications for the disease-initiating DNA expansion.

ACKNOWLEDGMENT

We are grateful to Prof. Gregory Verdine (Harvard University) and his laboratory for providing the expression plasmid for hOGG1 and to Dr. Wayne Chou and Prof. David Cane (Brown University) for assistance with protein expression and helpful discussion.

SUPPORTING INFORMATION AVAILABLE

Determination of active enzyme concentration, optical melting analysis of duplex and hairpin assemblies (with and without internal control region), autoradiogram revealing modification by DEPC and optical melting analysis for the mixed-sequence hairpin assembly, autoradiogram revealing modification of mixed-sequence hairpin assembly by peroxynitrite, autoradiogram revealing modification of $(CAG)_{10}$ hairpins with 8-oxoG in either the stem or loop by DEPC, graphical representation of hOGG1 time course data for the mixed-sequence duplex with and without NaOH/heat treatment, and autoradiogram revealing

strand scission of stem-HP and loop-HP by hOGG1 without NaOH/heat treatment. This material is available free of charge via the Internet at http://pubs.acs.org.

REFERENCES

1. Huntington's Disease Collaborative Research Group (1993) A novel gene containing a trinucleotide repeat that is expanded and unstable on Huntington's disease chromosomes. *Cell 72*, 971–983.
2. McMurray, C. T. (2001) Huntington's disease: new hope for therapeutics. *Trends Neurosci. 24*, S32–S38.
3. Cummings, C. J., and Zoghbi, H. Y. (2000) Trinucleotide repeats: mechanisms and pathophysiology. *Annu. Rev. Genomics Hum. Genet. 1*, 281–328.
4. Kovtun, I. V., and McMurray, C. T. (2008) Features of trinucleotide repeat instability *in vivo*. *Cell Res. 18*, 198–213.
5. Wells, R. D. (2007) Non-B DNA conformations, mutagenesis and disease. *Trends Biochem. Sci. 32*, 271–278.
6. Gacy, A. M., Goellner, G., Juranic, N., Macura, S., and McMurray, C. T. (1995) Trinucleotide repeats that expand in human disease form hairpin structures *in vitro*. *Cell 81*, 533–540.
7. Mitas, M. (1997) Trinucleotide repeats associated with human disease. *Nucleic Acids Res. 25*, 2245–2253.
8. Paiva, A. M., and Sheardy, R. D. (2004) Influence of sequence context and length on the structure and stability of triplet repeat DNA oligomers. *Biochemistry 43*, 14218–14227.
9. Kovtun, I. V., Liu, Y., Bjoras, M., Klugland, A., Wilson, S. H., and McMurray, C. T. (2007) OGG1 initiates age-dependent CAG trinucleotide expansion in somatic cells. *Nature 447*, 447–452.
10. David, S. S., O'Shea, V. L., and Kundu, S. (2007) Base-excision repair of oxidative DNA damage. *Nature 447*, 941–950.
11. Radicella, J. P., Dherin, C., Desmaze, C., Fox, M. S., and Boiteux, S. (1997) Cloning and characterization of *hOGG1*, a human homolog of the *OGG1* gene of *Saccharomyces cerevisiae*. *Proc. Natl. Acad. Sci. U. S.A. 94*, 8010–8015.
12. Beaucage, S. L., and Caruthers, M. H. (2000) Synthetic strategies and parameters involved in the synthesis of oligodeoxyribonucleotides according to the phosphoramidite method. *Curr. Protoc. Nucleic Acid Chem.* 3.3.1–3.3.20.
13. Warshaw, M. M., and Tinoco, I. Jr. (1966) Optical properties of sixteen dinucleoside phosphates. *J. Mol. Biol. 20*, 29–38.
14. Lymar, S. V., and Hurst, J. K. (1995) Rapid reaction between peroxonitrite ion and carbon dioxide: Implications for biological activity. *J. Am. Chem. Soc. 117*, 8867–8868.
15. Denicola, A., Freeman, B. A., Trujillo, M., and Radi, R. (1996) Peroxynitrite reaction with carbon dioxide/bicarbonate: Kinetics and influence on peroxynitrite-mediated oxidations. *Arch. Biochem. Biophys. 333*, 49–58.
16. Nash, H. M., Lu, R., and Verdine, G. L. (1997) The critical active-site amine of the human 8-oxoguanine DNA glycosylase, hOgg1: direct identification, ablation and chemical reconstitution. *Chem. Biol. 4*, 693–702.
17. Leipold, M. D., Workman, H., Muller, J. G., Burrows, C. J., and David, S. S. (2003) Recognition and removal of oxidized guanines in duplex DNA by the base excision repair enzymes hOGG1, yOGG1, and yOGG2. *Biochemistry 42*, 11373–11381.
18. Porello, S. L., Leyes, A. E., and David, S. S. (1998) Single-turnover and pre-steady-state kinetics of the reaction of the adenine glycosylase MutY with mismatch-containing DNA substrates. *Biochemistry 37*, 14756–14764.
19. Krishnamurthy, N., Haraguchi, K., Greenberg, M. M., and David, S. S. (2008) Efficient removal of formamidopyrimidines by 8-oxoguanine glycosylases. *Biochemistry 47*, 1043–1050.
20. Marky, L. A., and Breslauer, K. J. (1987) Calculating thermodynamic data for transitions of any molecularity from equilibrium melting curves. *Biopolymers 26*, 1601–1620.
21. Huertas, D., Bellsolell, L., Casasnovas, J. M., Coll, M., and Azorin, F. (1993) Alternating $d(GA)_n$ DNA sequences form antiparallel stranded homoduplexes stabilized by the formation of G.A base pairs. *EMBO J. 12*, 4029–4038.
22. Völker, J., Makube, N., Plum, G. E., Klump, H. H., and Breslauer, K. J. (2002) Conformational energetics of stable and metastable states formed by DNA triplet repeat oligonucleotides: Implications for triplet expansion diseases. *Proc. Natl. Acad. Sci. U.S.A. 99*, 14700–14705.
23. Steenken, S., and Jovanovic, S. V. (1997) How easily oxidizable is DNA? One-electron reduction potentials of adenosine and guanosine radicals in aqueous solution. *J. Am. Chem. Soc. 119*, 617–618.
24. Niles, J. C., Wishnok, J. S., and Tannenbaum, S. R. (2006) Peroxynitrite-induced oxidation and nitration products of guanine and 8-oxoguanine: Structures and mechanisms of product formation. *Nitric Oxide 14*, 109–121.
25. Shafirovich, V., Mock, S., Kolbanovskiy, A., and Geacintov, N. E. (2002) Photochemically catalyzed generation of site-specific 8-nitroguanine adducts in DNA by the reaction of long-lived neutral guanine radicals with nitrogen dioxide. *Chem. Res. Toxicol. 15*, 591–597.
26. Gu, F., Stillwell, W. G., Wishnok, J. S., Shallop, A. J., Jones, R. A., and Tannenbaum, S. R. (2002) Peroxynitrite-induced reactions of synthetic oligo 2′-deoxynucleotides and DNA containing guanine: Formation and stability of a 5-guanidino-4-nitroimidazole lesion. *Biochemistry 41*, 7508–7518.
27. Cullis, P. M., Malone, M. E., and Merson-Davies, L. A. (1996) Guanine radical cations are precursors of 7,8-dihydro-8-oxo-2'-deoxyguanosine but are not precursors of immediate strand breaks in DNA. *J. Am. Chem. Soc. 118*, 2775–2781.
28. David, S. S., and Williams, S. D. (1998) Chemistry of glycosylases and endonucleases involved in base-excision repair. *Chem. Rev. 98*, 1221–1262.
29. Ross, S. A., and Burrows, C. J. (1996) Cytosine-specific chemical probing of DNA using bromide and monoperoxysulfate. *Nucleic Acids Res. 24*, 5062–5063.
30. Hayatsu, H., and Ukita, T. (1967) The selective degradation of pyrimidines in nucleic acids by permanganate oxidation. *Biochem. Biophys. Res. Commun. 29*, 556–561.
31. Carter, P. J., Cheng, C. C., and Thorp, H. H. (1996) Oxidation of DNA hairpins by oxoruthenium(IV): effects of sterics and secondary structure. *Inorg. Chem. 35*, 3348–3354.
32. Lee, B. J., Barch, M., Castner, E. W. Jr., Völker, J., and Breslauer, K. J. (2007) Structure and dynamics in DNA looped domains: CAG triplet repeat sequence dynamics probed by 2-aminopurine fluorescence. *Biochemistry 46*, 10756–10766.
33. Dou, H., Mitra, S., and Hazra, T. K. (2003) Repair of oxidized bases in DNA bubble structures by human DNA glycosylases NEIL1 and NEIL2. *J. Biol. Chem. 278*, 49679–49684.
34. Bruner, S. D., Norman, D. P., and Verdine, G. L. (2000) Structural basis for recognition and repair of the endogenous mutagen 8-oxoguanine in DNA. *Nature 403*, 859–866.
35. Uliel, L., Weisman-Shomer, P., Oren-Jazan, H., Newcomb, T., Loeb, L. A., and Fry, M. (2000) Human Ku antigen tightly binds and stabilizes a tetrahelical form of the Fragile X syndrome $d(CGG)_n$ expanded sequence. *J. Biol. Chem. 275*, 33134–33141.
36. Owen, B. A., Yang, Z., Lai, M., Gajek, M., Badger, J. D., Hayes, J. J., Edelmann, W., Kucherlapati, R., Wilson, T. M., and McMurray, C. T. (2005) (CAG)(n)-hairpin DNA binds to Msh2-Msh3 and changes properties of mismatch recognition. *Nat. Struct. Mol. Biol. 12*, 663–670.